ANTHROPOGENIC CONTRIBUTION TO THE 2017 EARLIEST SUMMER ONSET IN SOUTH KOREA

Seung-Ki Min, Yeon-Hee Kim, In-Hong Park, Donghyun Lee, Sarah Sparrow, David Wallom, and Dáithí Stone

Large-ensemble RCM and GCM simulations suggest a significant anthropogenic contribution to the observed warmest May and earliest summer onset in South Korea, increasing the risk of its occurrence by 2–3 times.

INTRODUCTION. During May 2017, South Korea experienced the hottest recorded temperature since 1973 (the beginning of the observations from 45 stations; Fig. 1a). This was the culmination of four consecutive years of record-breaking May temperatures (Fig. 1b). Responding to the early heat, in 2015 the Korean Meteorological Administration (KMA) started to issue heat wave warnings throughout the year rather than only during June–September (KMA 2015). Based on multiple coupled climate models (CMIP5; see below) the probability of having an extremely hot May (exceeding +1.5 standard deviation; red dashed line in Fig. 1b) for four consecutive years is extremely low, corresponding to a 1-in-1000-yr event without anthropogenic forcing and a 1-in-100-yr event with anthropogenic influences (Fig. ES1). This is consistent with the results for consecutive global record-breaking temperatures (Mann et al. 2017).

The warmer May temperatures were observed across South Korea (Fig. 1a), with the station mean being 1.5°C higher than 1987–2010 climatology (17.2°C; note a short period for climatology due to the w@h model experiment; see below). The hottest May coincides with the earliest summer onset about 8 days earlier than climatology (as defined in the Data and methods section below; see the green line in Fig. 1b), exerting huge societal impacts for health, economy, and leisure activities (*Korea Herald*,[1] *Korea Times*[2]). Indeed, the correlation between Korea May temperature and summer onset day is very strong ($r = -0.78$). A simple analysis suggests that this relation is a result of an overall warming throughout the seasons rather than a shift in the seasonality (Fig. 1c). Warmer May and earlier summer onset were also observed over the northern China (Figs. 1d,e), with 2°C warmer and 8–10 days earlier onset than climatology (refer to Fig. ES2 for climatology patterns). This regional summer lengthening has important implications for the overall midlatitudes (e.g., for agriculture; Qian et al. 2016), in terms of systematic changes in the annual cycle (Park et al. 2018).

This study examines human contribution to the 2017 extreme May heat and the earliest summer onset in South Korea. To consider small spatial scales, we use high-resolution large-ensemble regional climate model (RCM) and global climate model (GCM) simulations available for the year 2017, each performed with and without anthropogenic forcings. The risk ratio (RR) and fraction of attributable risk (FAR) are analyzed to assess changes in the probabilities of occurrence of the extreme summer onset between the real and counterfactual worlds.

DATA AND METHODS. We use daily mean temperatures (Tmean) from 45 South Korean weather stations for 1973–2017. To check regional-scale responses, we use monthly surface air temperature from

AFFILIATIONS: Min, Kim, Park, and Lee—Division of Environmental Science and Engineering, Pohang University of Science and Technology, Pohang, South Korea; Sparrow and Wallom—Oxford e-Research Centre, Department of Engineering, University of Oxford, Oxford, United Kingdom; Stone—Global Climate Adaptation Partnership, Oxford, United Kingdom
CORRESPONDING AUTHOR: Seung-Ki Min, skmin@postech.ac.kr

DOI:10.1175/BAMS-D-18-0096.1

A supplement to this article is available online (10.1175/BAMS-D-18-0096.2)

[1] www.koreaherald.com/view.php?ud=20170623000779&ACE_SEARCH=1
[2] http://koreatimes.co.kr/www/news/biz/2017/05/602_228786.html

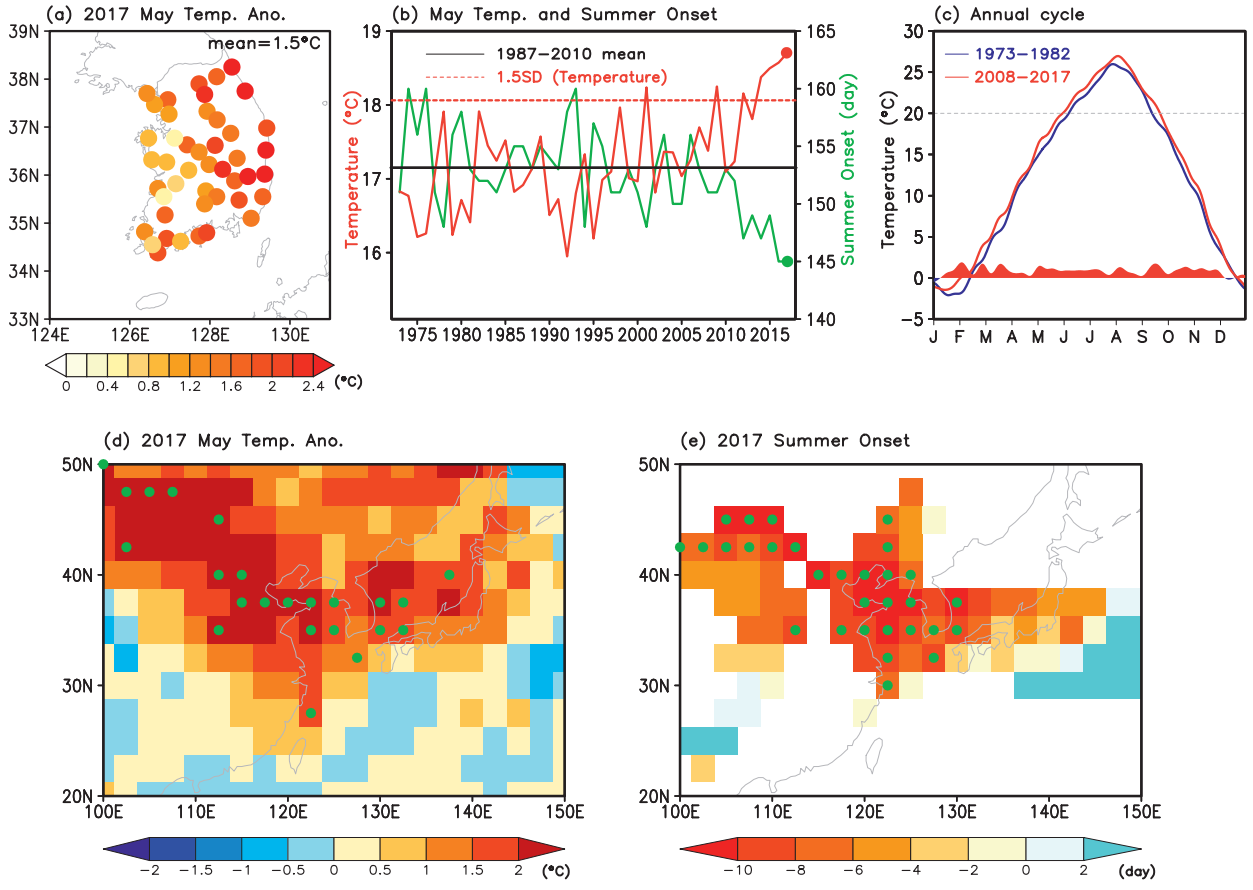

Fig. 1. (a) Distribution of May mean temperature anomalies observed at 45 stations over South Korea in 2017. Anomalies are with respect to 1987–2010 mean. (b) Time series of May mean temperature (red) and summer onset day (green) averaged over 45 stations for 1973–2017. Black solid line indicates 1987–2010 mean for both temperature and summer onset and red dashed line represents 1.5 standard deviation of temperature. (c) Annual cycle of South Korean temperature during 1973–82 and 2008–17 and their differences (red filled line). Also shown are the spatial distributions of (d) 2017 May mean temperature anomalies and (e) 2017 summer onset anomalies obtained from ERA-Interim reanalysis with 2.5° spatial resolution. In (e), areas are displayed only where May–June mean temperature are within 17°–23°C, having a similar summer onset to South Korea (see Fig. ES2b in the online supplemental information). Green dotted grids in (d) and (e) indicate the record high temperature and record early summer onset in 2017.

the ERA-Interim reanalysis. RCM data are obtained from the weather@home (w@h) East Asia project, which uses the HadRM3P RCM (the Hadley Centre Regional Climate Model, version 3, with improved physics parameterizations) nested in the HadAM3P atmospheric GCM (similar expansion; Massey et al. 2015; Guilliod et al. 2017). Observed sea surface temperature (SST), sea ice coverage, greenhouse gas, and aerosol were prescribed for the real world simulations (referred to as ALL). The counterfactual world simulations without human influences (NAT) were conducted with an adjusted SST, which was made by removing anthropogenic warming from the observed SST and using preindustrial levels of external forcings (see Table ES1 in the online supplemental material; Schaller et al. 2016). The RCM domain covers East Asia and Indian Ocean, consistent with Freychet et al. (2018), with a 50-km resolution. For GCM data, we use a large ensemble simulation of CAM5.1 that participated in the C20C+ D&A project, which was run at a resolution of 1° × 1° (Neale et al. 2012; Stone et al. 2018). The ALL and NAT simulations were conducted with prescribed observed and adjusted external forcings and boundary conditions, similarly to w@h experiment but with some differences (see Table ES1 for details). We also use the multimodel data from phase 5 of the Coupled Model Intercomparison Project (CMIP5; Taylor et al. 2012). RCP4.5 simulations for 2008–27 are used as ALL and natural forcing only runs for 1986–2005 are used as NAT (Table ES1). Anomalies for observations and all model data are calculated with respect to 1987–2010 means

(using ALL climatology for model data) to be matched with the data period from w@h runs.

The analysis domain for South Korea is 34°–38°N, 125°–130°E and a land–sea mask from each model is considered, regarding a grid with land fraction > 0.15 as land. Summer onset day is defined as the date with a smoothed May Tmean value over 20°C, which is determined adaptively and uniquely (Qian et al. 2009; 2011) by the ensemble empirical mode decomposition (EEMD) method (Wu and Huang 2009). All models used in this study can capture the observed summer onset day with Tmean of 20°C occurring during May–June (not shown). To quantify the anthropogenic contribution to the increased probability of occurrence of the extreme heat event, we analyze the risk ratio and fraction of attributable risk, which are defined as RR = P_{ALL}/P_{NAT} and FAR = 1 − (P_{NAT}/P_{ALL}), where P_{ALL} and P_{NAT} are probability of extreme events in ALL and NAT simulations, respectively (e.g., Easterling et al. 2016).

RESULTS. Figures 2a–c display frequency distributions of the Tmean and summer onset anomalies both individually (upper and right histograms) and combined (contours). The probability exceeding the observed value is calculated from fitted kernel distributions (using a Gaussian kernel function) for each variable. For w@h (Fig. 2a), the probability (P) of Tmean anomalies higher than the observed (+1.5°C) is 16.65% in ALL and 4.03% in NAT. For summer onset anomalies, P_{ALL} is also higher (32.55%) than P_{NAT} (12.17%). The resulting FAR values are 0.76 and 0.63, respectively (Table ES1), indicating a dominant contribution of anthropogenic forcings to the 2017-like extreme warming and early start of summer season. Joint probability exceeding the 2017 observations is found to be 9.86% in ALL and 2.79% in NAT, respectively. The corresponding FAR is 0.72 (RR = 3.53), indicating that the extreme risk increases about 3 to 4 times due to the anthropogenic forcing. CAM5.1 results (Fig. 2b) show that anthropogenic influences have increased the risk of extreme May Tmean and summer onset by about 17 times and 2–3 times, respectively (Table ES1). Results from CMIP5 are overall similar to those from w@h RCMs with FAR values being 0.89 and 0.63 for Tmean and summer onset, respectively (Fig. 2c). In conclusion, the 2017 record warm May and earliest summer start in South Korea are largely due to anthropogenic influences, at least doubling the likelihood (FAR > 0.5).

RR obtained from w@h, CAM5.1, and CMIP5 ensembles is summarized with corresponding uncertainty ranges (Figs. 2d,e). For May Tmean anomalies, all models show RR clearly above one, indicating that human influence is detectable. The stronger RR in CAM5.1 is related to its lower P_{NAT}, which seems to be associated with the smaller interensemble Tmean variability (Fig. 2b). The w@h simulations exhibit different RRs for Tmean according to different delta-SST patterns prescribed (ALL minus NAT; see Table ES2 for corresponding CMIP5 models). Results for summer onset show generally positive RR, which is relatively small compared to the Tmean case (Fig. 2e), with different RRs observed for different prescribed SSTs as well. Using the w@h ensemble, we examine the relationship between RR for Tmean and RR for summer onset (both on the logarithm scale). Results show a strong positive Tmean–summer onset relation (r = 0.90) in RR across different delta-SSTs (Fig. 2f), which represents influences of different CMIP5 models (see Table ES2). In this regard, a recent study found that intermodel spread in anthropogenic signals in South Korea is largely determined by intermodel spread in aerosol sensitivity (Kim et al. 2018). To check whether the same explanation can apply here, we compare the RR (log scale) from different delta-SST with the aerosol effective radiative forcing (AER) from the corresponding CMIP5 models (Fig. 2g). We find a statistically significant intermodel correlation (r = 0.74) such that models having larger cooling responses to aerosol forcing tend to have smaller RR and vice versa. Essentially identical results are observed between AER and delta-SST itself (not shown). This suggests an important role of aerosol cooling in determining uncertainties in the risk assessment over South Korea and possibly over East Asia. Further related analysis indicates a large difference in delta-SST patterns between w@h (weak) and CAM5.1 (strong; similar to CMIP5) ensembles (not shown). However, ALL–NAT differences in South Korean May Tmean are similar between the two models (around 0.7°–0.8°C; Figs. 2a,b), and this implies a stronger aerosol cooling effect in CAM5.1 than in w@h RCM (cf. Kim et al. 2018).

CONCLUDING REMARKS. The probability of an extremely warm May and unusually early summer onset in South Korea is compared between real world (ALL) and counterfactual world (NAT) conditions using the datasets from high-resolution large-ensemble simulations from an atmospheric RCM (w@h) and an atmospheric GCM (CAM5.1). Results with multiple coupled climate models (CMIP5) with a coarse resolution are also compared. All models consistently show increases in the likelihood of a 2017-like extreme event by about 2 to 3 times when including anthropogenic

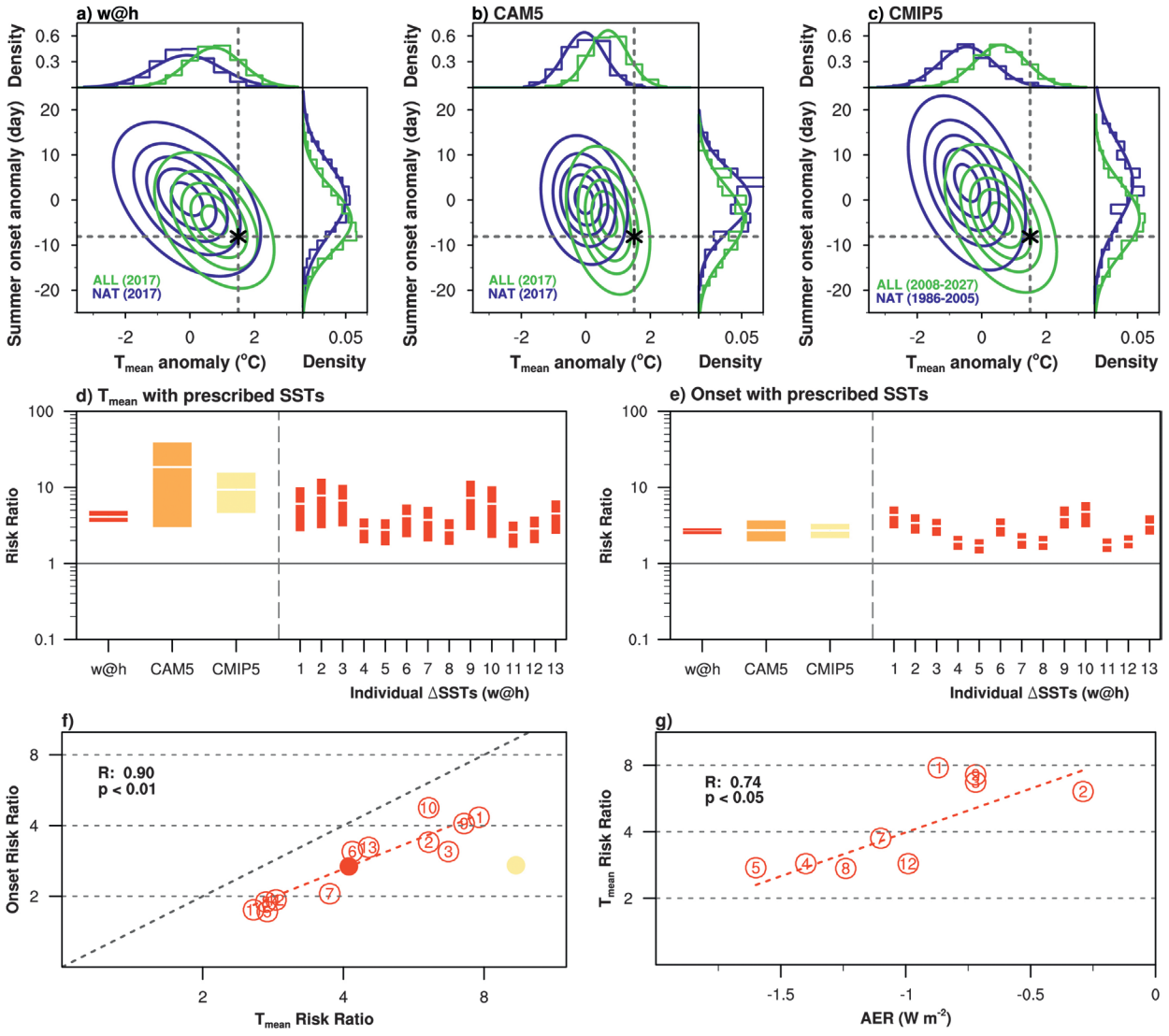

Fig. 2. Joint probability distribution of the May Tmean and summer onset anomalies form ALL (green) and NAT (blue) simulations from the (a) w@h, (b) CAM5, and (c) CMIP5 ensembles. Black asterisks and dashed lines represent observed values. Also shown are risk ratios for w@h, CAM5, and CMIP5 of (d) Tmean and (e) summer onset where left-hand side bars are from all simulations and right-hand side bars with numbers represent w@h results from different prescribed delta-SSTs (No. 1–12 obtained from different CMIP5 models and No. 13 with CMIP5 multimodel means as indicated in Table ES2). The 90% confidence interval of RR is estimated using the "basic bootstrap" method with 1,000 random samples (Paciorek et al. 2018) and the 90% confidence interval of the FAR is obtained by converting the log RR percentiles into FAR values. (f) Scatterplot between risk ratios of temperature and summer onsets. Red and yellow closed circles indicate w@h and CMIP5 ensemble means, respectively. (g) Scatterplot between for aerosol forcing [AER; obtained from Allen and Ajoku (2016)] and risk ratios of temperature. In (f) and (g), numbered circles represent values from w@h ensemble with different delta-SSTs as explained above.

forcing (mainly due to greenhouse gas increases). When repeating our analysis using a subset of CMIP5 models that provide both ALL and NAT runs (models marked with an asterisk in Table ES2), attribution results remain similar (not shown), indicating a weak influence of the different set of models for ALL and NAT runs. Further, it is suggested that differences in the attribution results among different boundary SSTs (or GCMs) are partly due to the intermodel difference in aerosol cooling effects, supporting previous findings. Our multimodel assessment provides a convincing evidence that human influence has contributed to the stronger and earlier heat wave by better considering intermodel uncertainties. Physical mechanisms responsible for the observed advance of summer onset and its uncertainty need to be further investigated.

ACKNOWLEDGMENTS. This work was supported by the Korea Meteorological Administration Research and Development Program under Grants KMI2018-03610 and KMA2018-00321 and by a National Research Foundation of Korea (NRF) grant funded by the Korean government (MSIT) (NRF-2018R1A5A1024958). This material is based upon work supported by the U.S. Department of Energy, Office of Science, Office of Biological and Environmental Research, under Contract DE-AC02-05CH11231.

REFERENCES

Allen, R. J., and O. Ajoku, 2016: Future aerosol reductions and widening of the northern tropical belt. *J. Geophys. Res.*, **121**, 6765–6786, https://doi.org/10.1002/2016JD024803.

Easterling, D. R., K. E. Kunkel, M. F. Wehner, and L. Sun, 2016: Detection and attribution of climate extremes in the observed record. *Wea. Climate Extremes*, **11**, 17–27, https://doi.org/10.1016/j.wace.2016.01.001.

Freychet, N., S. Sparrow, S. Tett, M. J. Mineter, G. Hegerl, and D. C. H. Wallom, 2018: Impacts of anthropogenic forcings and El Niño on Chinese extreme temperatures. *Adv. Atmos. Sci.*, **35**, 994–1002, https://doi.org/10.1007/s00376-018-7258-8.

Guilliod, B. P., and Coauthors, 2017: weather@home 2: Validation of an improved global–regional climate modeling system. *Geosci. Model Dev.*, **10**, 1849–1872, https://doi.org/10.5194/gmd-10-1849-2017.

Kim, Y.-H., S.-K. Min, D. A. Stone, H. Shiogama, and P. Wolski, 2018: Multi-model event attribution of the summer 2013 heat wave in Korea. *Wea. Climate Extremes*, **20**, 33–44, https://doi.org/10.1016/j.wace.2018.03.004.

KMA, 2015: Early heat wave warning issued throughout the year (in Korean). Korean Meteorological Administration, accessed 10 April 2018, http://web.kma.go.kr/notify/press/kma_list.jsp? bid=press&mode=view&num=1193019&page=1&field=subject&text=%C6%F8%BF%B0.

Mann, M. E., S. K. Miller, S. Rahmstorf, B. A. Steinman, and M. Tingley, 2017: Record temperature streak bears anthropogenic fingerprint. *Geophys. Res. Lett.*, **44**, 7936–7944, https://doi.org/10.1002/2017GL074056.

Massey, N., and Coauthors, 2015: weather@home—Development and validation of a very large ensemble modelling system for probabilistic event attribution. *Quart. J. Roy. Meteor. Soc.*, **141**, 1528–1545, https://doi.org/10.1002/qj.2455.

Neale, R. B., and Coauthors, 2012: Description of the NCAR Community Atmosphere Model (CAM 5.0). NCAR Tech. Note, NCAR/TN-486+STR, 289 pp., www.cesm.ucar.edu/models/cesm1.0/cam/docs/description/cam5_desc.pdf.

Paciorek, C. J., D. A. Stone, and M. F. Wehner, 2018: Quantifying uncertainty in the attribution of human influence on severe weather. *Wea. Climate Extremes*, **20**, 69–80, https://doi.org/10.1016/j.wace.2018.01.002.

Park, B.-J., Y.-H. Kim, S.-K. Min, and E.-P. Lim, 2018: Anthropogenic and natural contributions to the lengthening of the summer season in the Northern Hemisphere. *J. Climate*, **31**, 6803–6819, https://doi.org/10.1175/JCLI-D-17-0643.1.

Qian, C., C. Fu, Z. Wu, and Z. Yan, 2009: On the secular change of spring onset at Stockholm. *Geophys. Res. Lett.*, **36**, L12706, https://doi.org/10.1029/2009GL038617.

——, ——, ——, and ——, 2011: The role of changes in the annual cycle in earlier onset of climatic spring in northern China. *Adv. Atmos. Sci.*, **28**, 284–296, https://doi.org/10.1007/s00376-010-9221-1.

——, G. Ren, and Y. Zhou, 2016: Urbanization effects on climatic changes in 24 particular timings of the seasonal cycle in the middle and lower reaches of the Yellow River. *Theor. Appl. Climatol.*, **124**, 781–791, https://doi.org/10.1007/s00704-015-1446-6.

Schaller, N., and Coauthors, 2016: Human influence on climate in the 2014 southern England winter floods and their impacts. *Nat. Climate Change*, **6**, 627–634, https://doi.org/10.1038/nclimate2927.

Stone, D. A., and Coauthors, 2018: A basis set for exploration of sensitivity to prescribed ocean conditions for estimating human contributions to extreme weather in CAM5.1-1degree. *Wea. Climate Extremes*, **19**, 10–19, https://doi.org/10.1016/j.wace.2017.12.003.

Taylor, K. E., R. J. Stouffer, and G. A. Meehl, 2012: An overview of CMIP5 and the experiment design. *Bull. Amer. Meteor. Soc.*, **93**, 485–498, https://doi.org/10.1175/BAMS-D-11-00094.1.

Wu, Z., and N. E. Huang, 2009: Ensemble empirical mode decomposition: A noise-assisted data analysis method. *Adv. Adapt. Data Anal.*, **1**, 1–41, https://doi.org/10.1142/S1793536909000047.